How to cite: Angew. Chem. Int. Ed. 2023, e202308699
doi.org/10.1002/anie.202308699

Sodium-Metal Batteries

Single-Ion Conducting Polymer Electrolyte for Superior Sodium-Metal Batteries

Xu Dong, Xu Liu, Huihua Li, Stefano Passerini, and Dominic Bresser**

Abstract: Sodium-metal batteries (SMBs) are considered a potential alternative to high-energy lithium-metal batteries (LMBs). However, the high reactivity of metallic sodium towards common liquid organic electrolytes renders such battery technology particularly challenging. Herein, we propose a multi-block single-ion conducting polymer electrolyte (SIPE) doped with ethylene carbonate as suitable electrolyte system for SMBs. This novel SIPE provides a very high ionic conductivity (2.6 mS cm^{-1}) and an electrochemical stability window of about 4.1 V at 40 °C, enabling stable sodium stripping and plating and excellent rate capability of Na||$Na_3V_2(PO_4)_3$ cells up to 2 C. Remarkably, such cells provide a capacity retention of about 85 % after 1,000 cycles at 0.2 C thanks to the very high Coulombic efficiency (99.9 %), resulting from an excellent interfacial stability towards sodium metal and the $Na_3V_2(PO_4)_3$ cathode.

Low-cost and high-efficiency energy storage devices are considered key for the successful transition to renewable energy sources.[1] Over the past decades, lithium-based batteries have dominated the electrochemical energy storage market and are nowadays widely applied in portable electronics, (hybrid) electric vehicles, and also stationary storage systems.[2] However, this exceptional success also raised concerns about the availability of the elements and compounds required with regard to the essentially exponential rise in lithium battery sales, including lithium.[3] Therefore, batteries based on sodium cations as the charge carrier have attracted an increasing awareness, which very recently resulted in the announcement of several companies around the globe to commercialize sodium-ion batteries.[4] Among the key advantages of sodium batteries compared to lithium batteries are the almost unlimited abundance of sodium and its very homogeneous distribution around the world as well as the use of aluminum as current collector for both the electrodes.[3b,f,5] Their energy density, however, is significantly lower than that of lithium-ion batteries.[6] One possibility to address this issue might be the use of metallic sodium at the negative electrode, offering a high theoretical specific capacity of 1,165 mAh g^{-1} along with a low redox potential of −2.71 V vs. the standard hydrogen electrode.[7] Nevertheless, sodium-metal electrodes (similar to lithium-metal electrodes) suffer from the risk of dendritic sodium deposition and high reactivity with the conventional organic liquid electrolytes, which leads to continuous capacity loss and a relatively low Coulombic efficiency (CE).[8] The risk of dendrite formation is particularly pronounced at elevated currents approaching or even exceeding the limiting current density owing to the depletion of sodium cations at the negative electrode surface.[9] Once the dendrites have penetrated the separator and reached the opposite positive electrode, the resulting short circuit leads to severe safety issues.[10] One approach to overcome this issue relies on the design of single-ion conducting electrolytes with a sodium transference number (t_{Na+}) of (close to) unity, for which the Sand's time is theoretically approaching infinity.[9c,11] This can be realized in polymers, for instance, by covalently tethering the anionic group to the polymer backbone, leaving only the cation for the effective charge transport in the electrolyte.[12] Achieving sufficiently high ionic conductivity (> 0.1 mS cm^{-2}), though, is a great challenge in this case.[13]

Following our work on single-ion conducting polymer electrolytes (SIPEs) for lithium batteries,[14] we report herein a sodium SIPE doped with ethylene carbonate (EC) that shows a very high ionic conductivity and suitable electrochemical stability window. This SIPE enables the realization of Na||$Na_3V_2(PO_4)_3$ (NVP) cells providing very good rate capability and excellent cycling stability for 1,000 cycles.

The molecular structure of the multi-block copolymer sodium SIPE is given in Figure 1a. The synthesis is described in detail in the Supporting Information and involves essentially three steps, i.e., the synthesis of the polymer backbone (Figure S1), its bromination (Figure S2), and the attachment of the ionic side chains (Figure S3). The eventual structure comprises weakly coordinating anionic side chains in the ionophilic block, enabling a facile dissociation of the

[*] Dr. X. Dong, Dr. X. Liu, Dr. H. Li, Prof. S. Passerini, Dr. D. Bresser
Helmholtz Institute Ulm (HIU)
Helmholtzstrasse 11, 89081 Ulm (Germany)
and
Karlsruhe Institute of Technology (KIT)
P.O. Box 3640, 76021 Karlsruhe (Germany)
E-mail: stefano.passerini@kit.edu
dominic.bresser@kit.edu
Prof. S. Passerini
Chemistry Department, Sapienza University of Rome
Piazzale A. Moro 5, 00185 Rome (Italy)

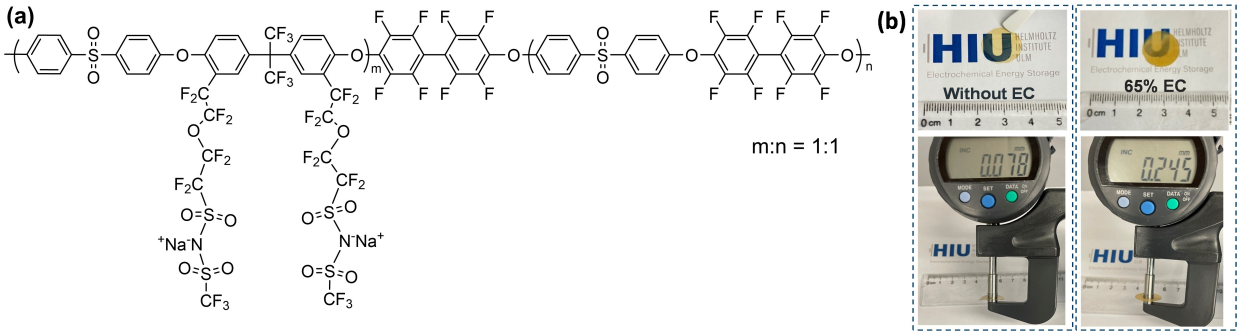

Figure 1. (a) Chemical structure of the sodium ionomer. (b) Photographs of the EC-free and EC-doped ionomer membranes with an indication of their thickness.

sodium cations, and rigid, nonpolar ionophobic blocks that are non-miscible with the ionophilic blocks, ensuring suitable mechanical properties and, thus, allowing for the realization of free-standing polymer membranes. The charge transport is further supported by the incorporation of small molecules with a high dielectric constant that can coordinate the sodium cations and by this lower the activation energy for the jump from one anionic site to another. Via solvent casting, transparent, uniform, and self-standing membranes with a thickness of around 80 µm were obtained (Figure 1b). These membranes were doped with 65 wt.% EC, which resulted in a significant increase in thickness by about 200 % (Figure 1b). The EC content was confirmed by thermogravimetric analysis (TGA), as depicted in Figure 2a (see also Figure S4 for pure EC as reference), revealing the EC evaporation prior to the thermal decomposition of the ionomer at about 400 °C. Figure 2b displays the differential scanning calorimetry (DSC) data. The DSC trace shows one

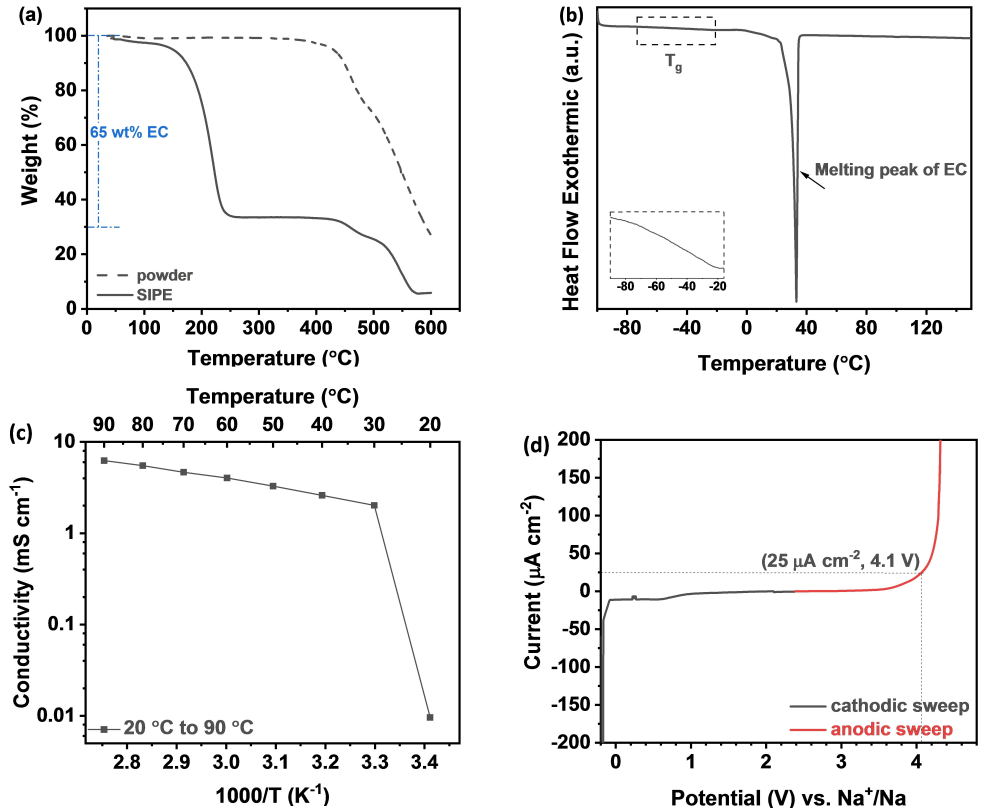

Figure 2. (a) TGA data recorded for the dry ionomer (dashed line) and the EC-doped membranes (solid line) with an indication of the EC content. (b) DSC thermogram recorded for the EC-doped ionomer membrane with an indication of the melting point of EC and the T_g (see also a magnification of the indicated region as inset; sweep rate: 5 °C min^{-1}). (c) Temperature-dependent ionic conductivity of the EC-doped ionomer. (d) LSV plot for the determination of the electrochemical stability with the cathodic sweep in black and the anodic sweep in red (sweep rate: 1 mV s^{-1}; temperature: 40 °C).

sharp endothermic peak at around 33 °C resulting from the melting of EC and a glass transition temperature (T_g) well below −20 °C, demonstrating good comparability with the T_g of earlier reported ionomers applied in LMBs.[14] The ionic conductivity as a function of temperature is shown in Figure 2c. Above 20 °C where the ionic conductivity is hampered by (partially) crystallized EC,[14a] it jumps to $>1\ mS\,cm^{-1}$. At 40 and 80 °C, for instance, the conductivity is as high as 2.6 and $5.5\ mS\,cm^{-1}$, respectively, which is comparable to conventional liquid electrolytes - not least with respect to the substantially lower Na^+ transference number of such liquid systems.[15] Similarly, a very high limiting current density of $5.2\ mA\,cm^{-2}$ was recorded at 40 °C (Figure S5), which is well above the lithium analogues of such SIPEs.[14,16] The electrochemical stability of the EC-doped SIPE was evaluated via linear sweep voltammetry at 40 °C (Figure 2d). Towards reduction, only a very low current below 0.8 V was observed, presumably resulting from the decomposition of EC at the interface with the sodium-metal electrode.[17] Towards oxidation, the current remains essentially zero before sharply increasing beyond 4 V. If we consider an evolving current of $25\ \mu A\,cm^{-2}$ as the threshold, an anodic stability of 4.1 V vs. Na^+/Na was found, which appears sufficiently wide for the combination with, e.g., NVP as a well-known sodium battery cathode material with a desodiation potential of about 3.4 V.[18]

In a first step, though, we evaluated the stability towards sodium-metal electrodes upon stripping and plating in symmetric Na||Na cells (Figure 3). The test with varying current densities ranging from 5 to $50\ \mu A\,cm^{-2}$ is depicted in Figure 3a along with a magnification of selected stripping/plating cycles for all current densities in Figure 3b. Gen-

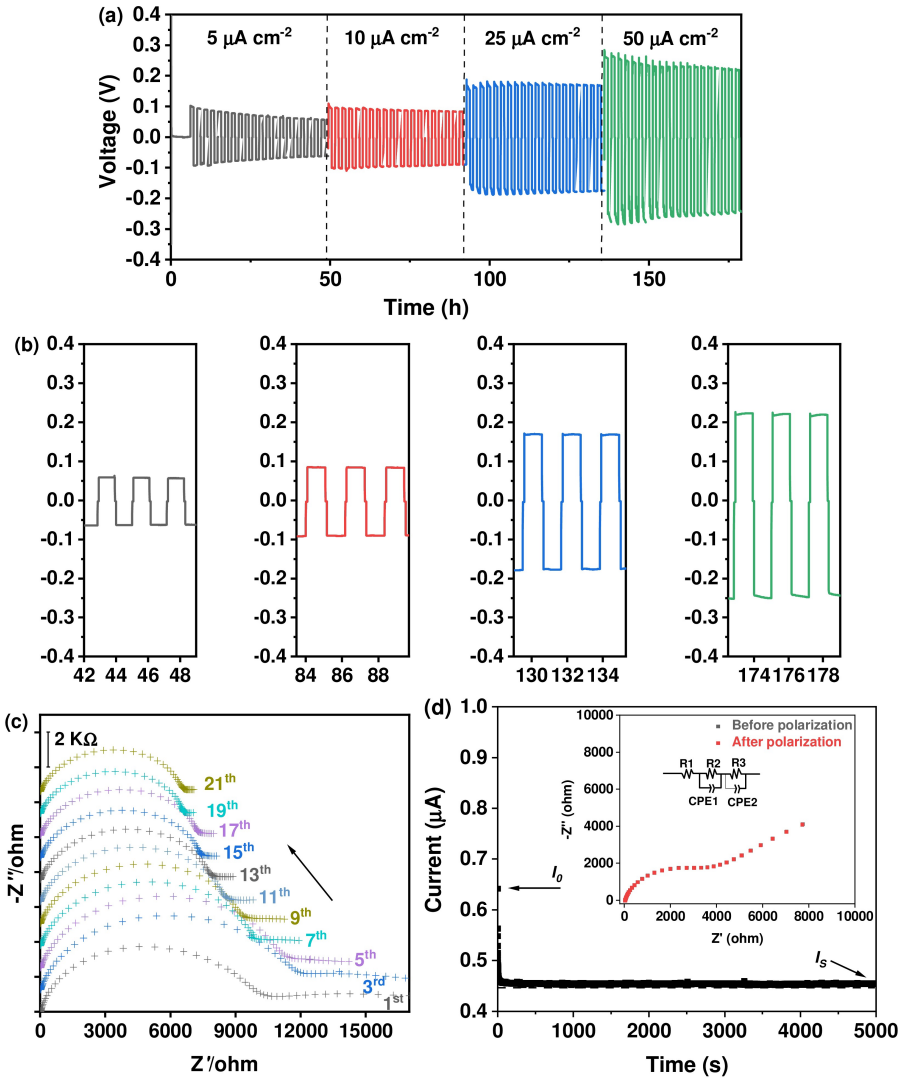

Figure 3. (a) Galvanostatic stripping and plating experiments conducted in symmetric Na||Na cells comprising the EC-doped ionomer as electrolyte at varying current densities at 40 °C. (b) Magnification of selected stripping/plating cycles at the different current densities. (c) Electrochemical impedance spectra recorded for symmetric Na||Na cells upon stripping and plating at a current density of $50\ \mu A\,cm^{-2}$ at 40 °C; impedance spectra were recorded each 10 stripping/plating cycles, i.e., 1st refers to 10 stripping/plating cycles, 3rd to 30 stripping/plating cycles etc.; for clarity reasons only each 2nd measurement is presented. (d) Determination of t_{Na+} via CA with the corresponding impedance spectra recorded before and after the CA experiment as inset along with the equivalent circuit used for the analysis.

erally, the overpotential remains rather stable independent of the applied current density, after an initial slight decrease in overpotential. This initial decrease appears to be related to an initial decrease in interfacial resistance, as revealed by an additional constant current stripping/plating experiment at 50 $\mu A\,cm^{-2}$ accompanied by continuous electrochemical impedance spectroscopy measurements each 10 stripping and plating cycles (Figure 3c). The interfacial impedance (R_i) first increases slightly from the 1st to the 3rd EIS measurement, before it continuously decreases upon further stripping and plating and eventually stabilizes after about 190 cycles at about 7,300 Ω along with a decrease and stabilization in overpotential (Figure S6). This stabilization indicates the formation of a stable interface (and presumably interphase) between the SIPE and the metallic sodium electrodes. The relatively high R_i can be attributed to the rather resistive interphase on the pristine sodium metal resulting from the processing of bulk sodium metal into foils as well as an interfacial contribution resulting from a spontaneous reaction between the EC-doped SIPE and the sodium-metal electrodes. This resistive interphase hinders the Na^+ ion transport across the interface, as also reflected by the generally rather high overpotential of up to about 0.2 V at 50 $\mu A\,cm^{-2}$, as also reported earlier for other sodium polymer electrolytes (Table S1). Nonetheless, the voltage response of the stripping/plating cycles remains very flat at each current density, as expected for a single-ion conducting electrolyte system. The single-ion conductivity was further confirmed by the determination of the cationic transference number according to the method reported by Bruce, Vincent and Evans,[19] revealing a value of 0.96 (Figure 3d), which is very close to unity. In fact, the current remains highly stable for 5,000 s and the impedance before and after polarization are very well overlapping, further indicating the formation of a stable electrode|electrolyte interface. Finally, we evaluated the performance of this SIPE in SMB configuration with NVP cathodes, i.e., in Na|SIPE|NVP cells (Figure 4). With regard to the ionic conductivity, the testing was conducted at 40 °C in order to ensure a high ionic conductivity of the SIPE in such cells. The active material mass loading was about 2.8 ± 0.1 $mg\,cm^{-2}$, and a C rate of 1 C corresponds to a specific current of 120 $mA\,g^{-1}$ and a current density of 0.336 $mA\,cm^{-2}$. Remarkably, the cells showed high specific capacities of 107 and 104 $mAh\,g^{-1}$ at 0.1 C and 1 C, respectively (Figure 4a). Even at 2 C, the cells still provided a very high reversible capacity of 100 $mAh\,g^{-1}$, which corresponds to about 94 % of the initial capacity at 0.05 C,

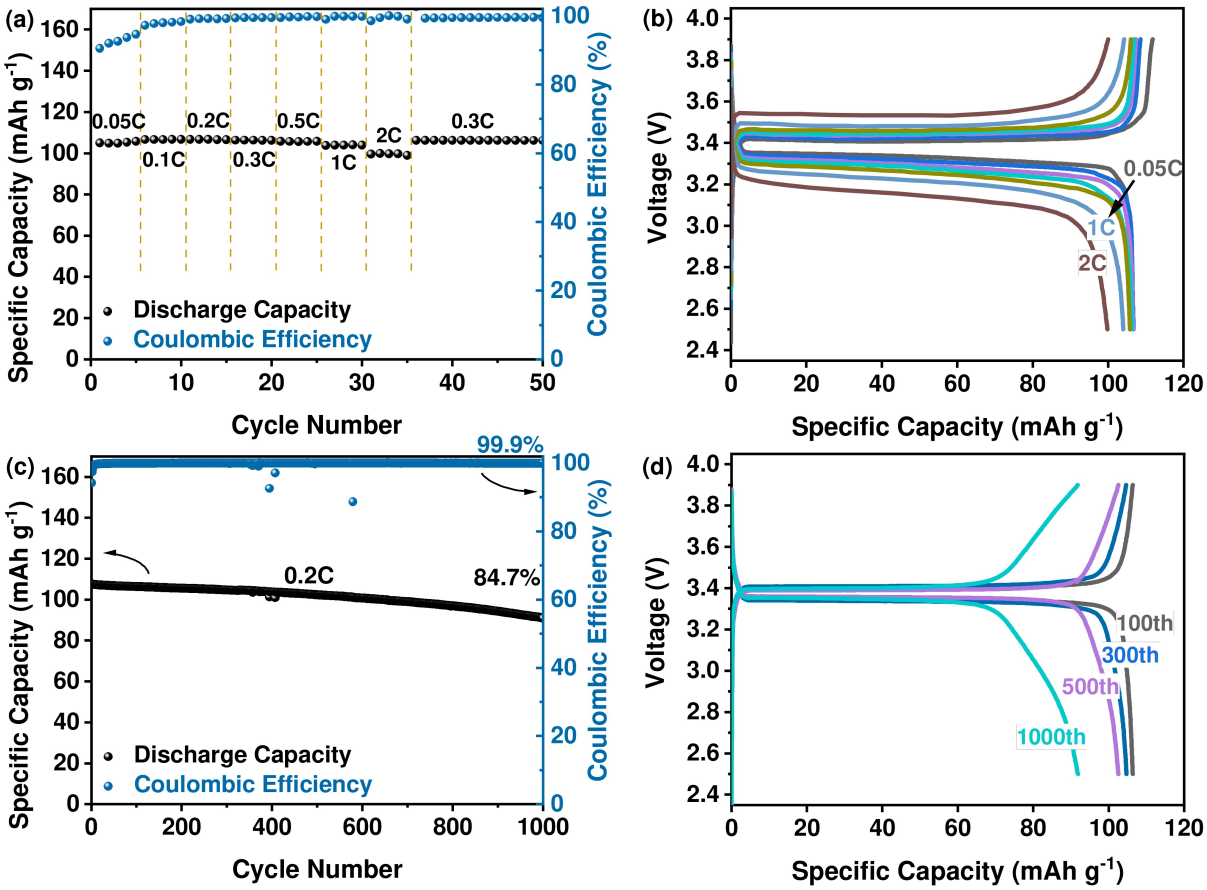

Figure 4. (a) Galvanostatic cycling of Na||NVP cells comprising the EC-doped ionomer as electrolyte at varying C rates (cut-off voltages: 2.5 and 3.9 V; temperature: 40 °C). (b) Selected dis-/charge profiles for the different C rates. (c) Constant current cycling of Na||NVP cells at 0.2 C (temperature: 40 °C). (d) Selected dis-/charge profiles of the 100th, 300th, 500th, and 1000th cycle.

indicating an excellent rate capability of such cells. When the dis-/charge rate was decreased back to 0.3 C, a specific capacity of 106 mAh g^{-1} was obtained, i.e., exactly the same capacity as prior to the application of the elevated dis-/charge rates. The corresponding dis-/charge profiles for the different C rates are presented in Figure 4b, and it can be seen that the polarization is generally very low and increases only slightly when increasing the dis-/charge rate from 0.05 C to 2 C, i.e., by a factor of 40. Additionally, we evaluated the long-term cycling stability of these Na|SIPE|NVP cells by subjecting them to 1,000 cycles at 0.2 C (Figure 4c). The cells displayed a very stable cycling with only minor capacity fading, resulting in a capacity retention of 84.7 % after 1,000 cycles (i.e., 91 mAh g^{-1} compared to the initial reversible specific capacity of 107 mAh g^{-1}). This stable cycling is not least the result of the exceptional average Coulombic efficiency of 99.9 %, which is a remarkably high value for sodium-metal cells. The comparison of selected dis-/charge profiles, depicted in Figure 4d, reveals that there is no apparent increase in polarization upon cycling. Instead, the voltage plateau gets shorter and the region beyond the plateau gets more sloped, indicating presumably a degradation of the active material - potentially at the outer surface, thus, rendering the de-/sodiation process more sluggish. Nonetheless, the results show that such SIPE is a promising candidate for long-term stable, high-performance SMBs.

In summary, a new sodium SIPE doped with ethylene carbonate has been synthesized and studied as electrolyte for sodium-metal batteries. The self-standing SIPE membranes are characterized by a high ionic conductivity of 2.6 mS cm^{-1} at 40 °C, a cationic transference number of essentially unity, and an electrochemical stability window of $>$4 V. Benefitting from a very stable interface with sodium metal and an average Coulombic efficiency of 99.9 %, Na|SIPE|NVP cells showed a capacity retention of about 85 % after 1,000 cycles at 0.2 C and excellent rate capability with still 100 mAh g^{-1} at 2 C. The results show that polymer electrolytes are not only a suitable alternative to liquid electrolytes for lithium-metal batteries, but also for sodium-metal batteries.

Supporting Information

Experimental details and synthesis procedures, including ^{1}H and ^{19}F NMR spectra of the ionomer and its intermediates; TGA data recorded for pure EC as reference; determination of the limiting current density for the EC-doped ionomer membranes at 40 °C.

Acknowledgements

The authors would like to acknowledge financial support by the Federal Ministry of Education and Research (BMBF) within the HyPerium project (03XP0403C), as well as the financial support by the Helmholtz Association. Open Access funding enabled and organized by Projekt DEAL.

Conflict of Interest

The authors declare no conflict of interest.

Data Availability Statement

The data that support the findings of this study are available from the corresponding author upon reasonable request.

Keywords: Battery · $Na_3V_2(PO_4)_3$ · Polymer Electrolyte · Single-Ion Conductor · Sodium Metal

[1] a) Q. Zhao, X. Liu, S. Stalin, K. Khan, L. A. Archer, *Nat. Energy* **2019**, *4*, 365–373; b) A. S. Arico, P. Bruce, B. Scrosati, J.-M. Tarascon, W. Van Schalkwijk, *Materials for sustainable energy: a collection of peer-reviewed research and review articles from Nature Publishing Group* **2011**, 148–159; c) C. Liu, F. Li, L. P. Ma, H. M. Cheng, *Adv. Mater.* **2010**, *22*, E28-E62.

[2] a) H. Wang, E. Matios, J. Luo, W. Li, *Chem. Soc. Rev.* **2020**, *49*, 3783–3805; b) X. Zheng, C. Bommier, W. Luo, L. Jiang, Y. Hao, Y. Huang, *Energy Storage Mater.* **2019**, *16*, 6–23; c) C. Grey, J. Tarascon, *Nat. Mater.* **2017**, *16*, 45–56.

[3] a) E. A. Olivetti, G. Ceder, G. G. Gaustad, X. Fu, *Joule* **2017**, *1*, 229–243; b) C. Vaalma, D. Buchholz, M. Weil, S. Passerini, *Nat. Rev. Mater.* **2018**, *3*, 18013; c) M. Armand, J.-M. Tarascon, *Nature* **2008**, *451*, 652–657; d) E. Matios, H. Wang, C. Wang, W. Li, *Ind. Eng. Chem. Res.* **2019**, *58*, 9758–9780; e) D. Larcher, J.-M. Tarascon, *Nat. Chem.* **2015**, *7*, 19–29; f) Y. Wang, Y. Wang, Y.-X. Wang, X. Feng, W. Chen, X. Ai, H. Yang, Y. Cao, *Chem* **2019**, *5*, 2547–2570.

[4] a) A. Rudola, A. J. Rennie, R. Heap, S. S. Meysami, A. Lowbridge, F. Mazzali, R. Sayers, C. J. Wright, J. Barker, *J. Mater. Chem. A* **2021**, *9*, 8279–8302; b) A. Bauer, J. Song, S. Vail, W. Pan, J. Barker, Y. Lu, *Adv. Energy Mater.* **2018**, *8*, 1702869; c) L. Zhao, T. Zhang, W. Li, T. Li, L. Zhang, X. Zhang, Z. Wang, *Engineering* **2022**, https://10.1016/j.eng.2021.08.032.

[5] a) R. Cao, K. Mishra, X. Li, J. Qian, M. H. Engelhard, M. E. Bowden, K. S. Han, K. T. Mueller, W. A. Henderson, J.-G. Zhang, *Nano Energy* **2016**, *30*, 825–830; b) W. Ling, N. Fu, J. Yue, X. X. Zeng, Q. Ma, Q. Deng, Y. Xiao, L. J. Wan, Y. G. Guo, X. W. Wu, *Adv. Energy Mater.* **2020**, *10*, 1903966; c) J. Zheng, S. Chen, W. Zhao, J. Song, M. H. Engelhard, J.-G. Zhang, *ACS Energy Lett.* **2018**, *3*, 315–321; d) C. Zhou, S. Bag, V. Thangadurai, *ACS Energy Lett.* **2018**, *3*, 2181–2198; e) Y. Tian, Y. Sun, D. C. Hannah, Y. Xiao, H. Liu, K. W. Chapman, S.-H. Bo, G. Ceder, *Joule* **2019**, *3*, 1037–1050.

[6] a) N. Yabuuchi, K. Kubota, M. Dahbi, S. Komaba, *Chem. Rev.* **2014**, *114*, 11636–11682; b) J.-Y. Hwang, S.-T. Myung, Y.-K. Sun, *Chem. Soc. Rev.* **2017**, *46*, 3529–3614.

[7] a) Y.-J. Kim, H. Lee, H. Noh, J. Lee, S. Kim, M.-H. Ryou, Y. M. Lee, H.-T. Kim, *ACS Appl. Mater. Interfaces* **2017**, *9*, 6000–6006; b) Z. W. Seh, J. Sun, Y. Sun, Y. Cui, *ACS Cent. Sci.* **2015**, *1*, 449–455; c) S. Wei, S. Choudhury, J. Xu, P. Nath, Z. Tu, L. A. Archer, *Adv. Mater.* **2017**, *29*, 1605512; d) Y. Yao, Z. Wei, H. Wang, H. Huang, Y. Jiang, X. Wu, X. Yao, Z. S. Wu, Y. Yu, *Adv. Energy Mater.* **2020**, *10*, 1903698.

[8] a) M. D. Slater, D. Kim, E. Lee, C. S. Johnson, *Adv. Funct. Mater.* **2013**, *23*, 947–958; b) M.-C. Bay, R. Grissa, K. V. Egorov, R. Asakura, C. Battaglia, *Mater. Futures* **2022**, *1*, 031001; c) H. Wan, J. P. Mwizerwa, X. Qi, X. Liu, X. Xu, H. Li, Y.-S. Hu, X. Yao, *ACS Nano* **2018**, *12*, 2809–2817.

[9] a) L. Yang, Y. Jiang, X. Liang, Y. Lei, T. Yuan, H. Lu, Z. Liu, Y. Cao, J. Feng, *ACS Appl. Energ. Mater.* **2020**, *3*, 10053–10060; b) Q. Ma, H. Zhang, C. Zhou, L. Zheng, P. Cheng, J. Nie, W. Feng, Y. S. Hu, H. Li, X. Huang, *Angew. Chem. Int. Ed.* **2016**, *55*, 2521–2525; c) P. Bai, J. Li, F. R. Brushett, M. Z. Bazant, *Energy Environ. Sci.* **2016**, *9*, 3221–3229.

[10] a) B. Lee, E. Paek, D. Mitlin, S. W. Lee, *Chem. Rev.* **2019**, *119*, 5416–5460; b) W. Luo, C. F. Lin, O. Zhao, M. Noked, Y. Zhang, G. W. Rubloff, L. Hu, *Adv. Energy Mater.* **2017**, *7*, 1601526; c) Y. Zhao, L. V. Goncharova, A. Lushington, Q. Sun, H. Yadegari, B. Wang, W. Xiao, R. Li, X. Sun, *Adv. Mater.* **2017**, *29*, 1606663; d) L. Shen, S. Deng, R. Jiang, G. Liu, J. Yang, X. Yao, *Energy Storage Mater.* **2022**, *46*, 175–181; e) H. Wan, J. P. Mwizerwa, F. Han, W. Weng, J. Yang, C. Wang, X. Yao, *Nano Energy* **2019**, *66*, 104109; f) H. Wan, W. Weng, F. Han, L. Cai, C. Wang, X. Yao, *Nano Today* **2020**, *33*, 100860.

[11] H. Zhang, C. Li, M. Piszcz, E. Coya, T. Rojo, L. M. Rodriguez-Martinez, M. Armand, Z. Zhou, *Chem. Soc. Rev.* **2017**, *46*, 797–815.

[12] a) M. D. Tikekar, S. Choudhury, Z. Tu, L. A. Archer, *Nat. Energy* **2016**, *1*, 16114; b) H. O. Ford, C. Cui, J. L. Schaefer, *Batteries* **2020**, *6*, 11; c) H. B. Youcef, B. Orayech, J. M. L. Del Amo, F. Bonilla, D. Shanmukaraj, M. Armand, *Solid State Ionics* **2020**, *345*, 115168.

[13] a) L. Yan, C. Rank, S. Mecking, K. I. Winey, *J. Am. Chem. Soc.* **2020**, *142*, 857–866; b) W. Zhang, S. Feng, M. Huang, B. Qiao, K. Shigenobu, L. Giordano, J. Lopez, R. Tatara, K. Ueno, K. Dokko, *Chem. Mater.* **2021**, *33*, 524–534; c) S. A. M. Noor, J. Sun, D. R. MacFarlane, M. Armand, D. Gunzelmann, M. Forsyth, *J. Mater. Chem. A* **2014**, *2*, 17934–17943.

[14] a) H.-D. Nguyen, G.-T. Kim, J. Shi, E. Paillard, P. Judeinstein, S. Lyonnard, D. Bresser, C. Iojoiu, *Energy Environ. Sci.* **2018**, *11*, 3298–3309; b) X. Dong, A. Mayer, X. Liu, S. Passerini, D. Bresser, *ACS Energy Lett.* **2023**, *8*, 1114–1121.

[15] D. Morales, L. G. Chagas, D. Paterno, S. Greenbaum, S. Passerini, S. Suarez, *Electrochim. Acta* **2021**, *377*, 138062.

[16] Z. Chen, D. Steinle, H.-D. Nguyen, J.-K. Kim, A. Mayer, J. Shi, E. Paillard, C. Iojoiu, S. Passerini, D. Bresser, *Nano Energy* **2020**, *77*, 105129.

[17] J. Zhang, D. W. Wang, W. Lv, L. Qin, S. Niu, S. Zhang, T. Cao, F. Kang, Q. H. Yang, *Adv. Energy Mater.* **2018**, *8*, 1801361.

[18] H. Zhang, B. Qin, D. Buchholz, S. Passerini, *ACS Appl. Energ. Mater.* **2018**, *1*, 6425–6432.

[19] J. Evans, C. A. Vincent, P. G. Bruce, *Polymer* **1987**, *28*, 2324–2328.

Manuscript received: June 20, 2023
Accepted manuscript online: July 26, 2023
Version of record online: ■■, ■■

Communications

Sodium-Metal Batteries

X. Dong, X. Liu, H. Li, S. Passerini,*
D. Bresser* ——— **e202308699**

Single-Ion Conducting Polymer Electrolyte for Superior Sodium-Metal Batteries

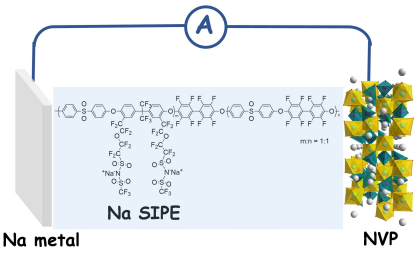

A new sodium single-ion conducting polymer electrolyte (SIPE) enables high rate capability and stable cycling of $Na||Na_3V_2(PO_4)_3$ (NVP) cells with an average Coulombic efficiency of 99.9% and a capacity retention of more than 84% after 1,000 cycles.